ENHANCING 1540 NM LIGHT EMISSION FROM ERBIUM DOPED STRONTIUM SUBSTITUTED HYDROXYAPATITE/BETA-TRICALCIUM PHOSPHATE

Le Thi Tam[1], Dao Hong Bach[1], Nguyen Duc Trung Kien[2], Truong Quoc Phong[1], Mai Xuan Dung[3], Truong Nguyen Tuan Minh[4], Le Tien Ha[5], Pham Hung Vuong[1*]
[1]Hanoi University of Science and Technology, [2]Phenikaa University, [3]Hanoi Pedagogical University 2, [4]Tampere University, Finland, [5]TNU - University of Science

ARTICLE INFO

Received: 05/8/2024
Revised: 26/11/2024
Published: 27/11/2024

KEYWORDS

Biomaterials
Luminescence
Hydroxyapatite
Erbium
Nanophosphors

ABSTRACT

This paper presents a method for synthesizing erbium (Er) doped strontium (Sr) substituted hydroxyapatite (HA)/hydroxyapatite/beta-tricalcium phosphate (TCP) nanostructures to achieve strong and stable near-infrared light emission at approximately 1540 nm. The Er-doped Sr-HA/TCP exhibited a rod-like structure by optimizing the concentrations of strontium and erbium and the annealing temperatures. The photoluminescence (PL) intensity of the sample increased with higher Sr and Er concentrations. The PL spectra of the nanoparticles displayed the characteristic luminescence of Er^{3+} centered at 1540 nm, which was more efficient in the annealed Er- doped Sr-HA/TCP compared to the annealed Er-doped HA/TCP nanoparticles. These findings indicate the potential of using Sr as a sensitizing material for synthesizing of Er-doped Sr-HA/TCP with strong 1540 nm light emission, suitable for applications in waveguide telecommunication and biomedicine.

TĂNG CƯỜNG PHÁT XẠ ÁNH SÁNG 1540 NM CỦA STRONTI THAY THẾ HYDROXYAPATITE/BETA-TRICALCIUM PHOSPHATE PHA TẠP ERBI

Lê Thị Tâm[1], Đào Hồng Bách[1], Nguyễn Đức Trung Kiên[2], Trương Quốc Phong[1], Mai Xuân Dũng[3], Trương Nguyễn Tuấn Minh[4], Lê Tiến Hà[5], Phạm Hùng Vượng[1*]
[1]Đại học Bách khoa Hà Nội, [2]Trường Đại học Phenikaa, [3]Trường Đại học Sư phạm Hà Nội 2 [4]Đại học Tampere University, Phần Lan, [5]Trường Đại học Khoa học - ĐH Thái Nguyên

THÔNG TIN BÀI BÁO

Ngày nhận bài: 05/8/2024
Ngày hoàn thiện: 26/11/2024
Ngày đăng: 27/11/2024

TỪ KHÓA

Vật liệu y sinh
Phát quang
Hydroxyapatite
Erbi
Nano-phốt pho

TÓM TẮT

Bài báo này trình bày một phương pháp tổng hợp vật liệu stronti thay thế vật liệu nano hydroxyapatite (HA)/hydroxyapatite/beta-tricalcium phosphate (TCP) pha tạp erbi (Er) để đạt được khả năng tăng cường phát xạ ánh sáng hồng ngoại gần ở khoảng 1540 nm. Bằng cách tối ưu hóa nồng độ stronti và erbi, cũng như nhiệt độ ủ, Sr-HA/TCP pha tạp Er cho thấy cấu trúc hình thanh. Cường độ phát quang (PL) của mẫu tăng khi nồng độ Sr và Er tăng lên. Phổ PL của các hạt nano cho thấy độ phát quang đặc trưng của Er^{3+} tập trung ở 1540 nm, hiệu quả hơn ở các hạt nano Sr-HA/TCP pha tạp Er so với các hạt nano HA/TCP pha tạp Er. Những phát hiện này cho thấy tiềm năng sử dụng Sr làm vật liệu tăng nhạy để tổng hợp Sr-HA/TCP pha tạp Er với khả năng phát xạ ánh sáng mạnh vùng 1540 nm cho các ứng dụng trong viễn thông ống dẫn sóng và y sinh học.

DOI: https://doi.org/10.34238/tnu-jst.10869

* Corresponding author. *Email: vuong.phamhung@hust.edu.vn*

1. Introduction

Erbium (Er)-doped materials have become crucial materials for applications such as optical communication, given that the transition from the first excited level $^4I_{13/2}$ to the ground state $^4I_{15/2}$ produces a light emission at around 1540 nm, a wavelength used in the telecommunication band for transmission of information [1], [2]. Despite advancements in synthesizing Er-doped waveguides, their practical application remains limited due to their low incorporation efficiency, concentration, and thermal quenching effect. This has driven scientists and engineers to seek new methods to precisely control and tailor the microstructure and physical characteristics of materials. For instance, to address new functional material, one approach is to insert the sensitized materials into host materials [3], [4]. Significant efforts have been made to enhance near-infrared luminescence by incorporating various sensitizing materials into Er-doped materials, such as nano silicon [5], [6], ytterbium (Yb) [7], [8], and germanium oxide (GeO_2) [9].

Compared to other host matrices, hydroxyapatite (HA; $Ca_{10}(PO_4)_6(OH)_2$) and beta-tricalcium phosphate (TCP; $Ca_3(PO_4)_2$) are suitable hosts for rare earth elements (RE) due to their flexible apatite structure [10], [11]. Additionally, strontium-substituted hydroxyapatite/TCP (Sr-HA/TCP) forms a solid solution with HA/TCP by replacing Ca^{2+} with Sr^{2+} over a wide range of concentrations [12], [13]. Sr-HA/TCP has garnered significant attention in engineered materials due to its acceleration of mineralization and crystallization of calcium phosphate in bone formation which is comparable to HA/TCP [14], [15]. These materials have been utilized in optical engineering to synthesize red and blue luminescent materials, showing high efficiency in luminescent HA/TCP [16], [17]. Recently, Er-doped hydroxyapatite (HA)/TCP was successfully synthesized in our laboratory using the co-precipitation method [18]. In that study, we examined the effect of thermal annealing on the near-infrared emission of Er-doped HA/TCP. To further this research, we report for the first time the strong near-infrared emission at about 1540 nm of strontium-substituted hydroxyapatite/TCP (Sr-HA/TCP) as a function of strontium, erbium concentration, and thermal annealing. The crystalline structures of Er-doped Sr-HA/TCP were characterized by X-ray diffraction (XRD), while the microstructure and chemical composition were analyzed using transmission electron microscopy (TEM) and energy dispersive X-ray spectroscopy (EDS), respectively. The light emission properties were determined using a photoluminescence spectrometer.

2. Experimental procedure

Erbium-doped Sr-HA/TCP was synthesized using a coprecipitation method. Specifically, a stoichiometric amount of $(NH_4)_2$ HPO_4 (0.2M, 99.9% purity, Aldrich) in aqueous solution was added to an aqueous solution containing Ca $(NO_3)_2$ $.4H_2O$ (0.2M, 99.9% purity, Aldrich) with varying amounts of $ErCl_3.6H_2O$ (99.9% purity, Aldrich) and $Sr(NO_3)_2$ (99.9% purity, Aldrich) under vigorous stirring. The reaction mixture was stirred for 0.5 hours, followed by precipitation at 80°C, with the pH adjusted to 11 using aqueous ammonia. The resulting precipitates were washed three times and then dried at 100°C for 6 hours. Portions of each as-prepared sample were treated at 600°C, 800°C, 1000°C, and 1100°C for 1 hour in air. The crystalline structures of the Er-doped Sr-HA/TCP were characterized using X-ray diffraction (XRD, D8 Advance, Bruker, Germany). The microstructure and chemical composition were determined by transmission electron microscopy (TEM, JEOL JEM 1010, JEOL Techniques, Tokyo, Japan) and field emission scanning electron microscopy (FESEM, JEOL JSM-6700F, JEOL Techniques, Tokyo, Japan). Photoluminescence (PL) tests were conducted to evaluate the optical properties using a NANO LOG spectrofluorometer (Horiba, USA) equipped with a 450 W Xe arc lamp and double excitation monochromators. The PL spectra were recorded automatically during the measurements.

3. Results and discussion

3.1. Phase characterization

Figures 1 display the XRD diagrams of Er-doped HA and Er-doped Sr-HA/TCP annealed at 800°C. All three XRD patterns exhibit a mixture of hydroxyapatite (PDF 09-0432) and β-tricalcium phosphate (β-TCP) (PDF 09-0169) with good crystallinity (Figure 1 (a)-(b)). The absence of any phases related to Er or Sr species in the XRD diagrams of the Er-doped HA/TCP and Er-doped Sr-HA/TCP specimens indicates the successful preparation of these materials. Additionally, HA containing HPO_4^{2-} ions converts to pyrophosphate ions ($P_2O_7^{4-}$) when heated to around 650°C [19], [20]. The $P_2O_7^{4-}$ ions then react with hydroxyl (OH-) ions, forming β-TCP during the thermal annealing process [21], [22]. The presence of a mixture of HA and β-TCP in the specimens suggests improved performance in optical materials due to the strong light emission properties of β-TCP [23], [24].

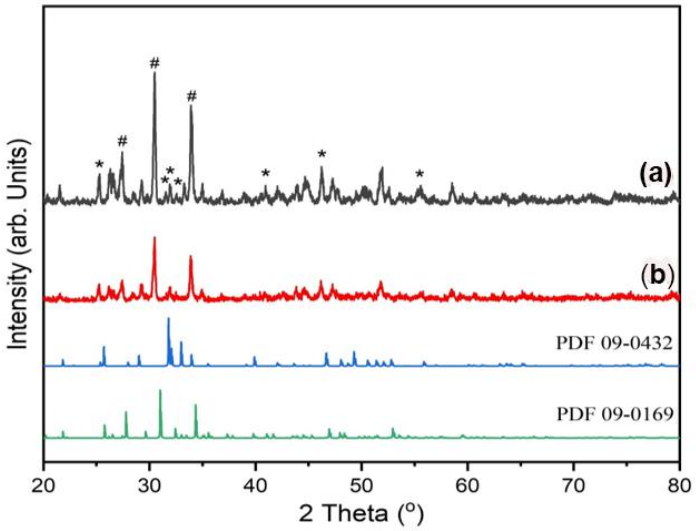

Figure 1. *XRD patterns of nanoparticle annealed at 800 °C (a) Er-doped HA/TCP and (b) Er-doped Sr-HA/TCP (*: HA and #: β-TCP)*

3.2. Scanning electron analysis

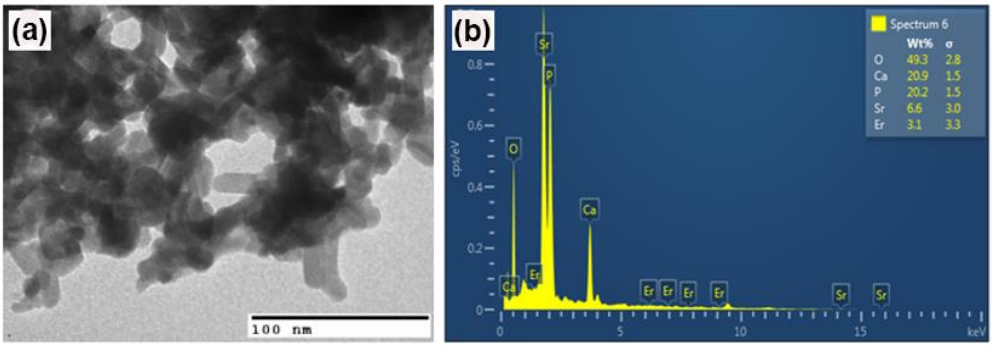

Figure 2. *Microanalysis of the Er-doped Sr-HA/TCP annealed at 800 °C (a) TEM image and (b) EDS analysis of chemical composition of specimens*

The representative microstructure and chemical composition of the Er-doped Sr-HA/TCP were analyzed using TEM and EDS, as depicted in Figures 2 (a) and (b). The specimen exhibited a rod-like microstructure with a diameter of approximately 30 nm (Figure 2(a)). Peaks corresponding to Sr and Er elements were observed (Figure 2(b)), confirming their presence in

the HA/TCP. Furthermore, the calculated weight concentrations of Sr and Er were approximately 6.6% and 3.1%, respectively, indicating the successful incorporation of Sr and Er ions into the host HA/TCP.

3.3. Effect of strontium concentrations

Figure 3 displays the photoluminescence spectra of Er-doped Sr-HA/TCP with varying Sr concentrations, annealed at 800°C. The spectra reveal strong near-infrared emission peaks around 1540 nm, attributed to the transition from the first excited level $^4I_{13/2}$ to the ground state $^4I_{15/2}$ within the 4f electronic configuration. Notably, the PL intensities of Er-doped Sr-HA/TCP increased along with the rising of Sr concentrations, peaking at 0.5% mol Sr, before decreasing with further higher Sr concentrations. The substitution of calcium (Ca) with strontium (Sr) leads to lattice expansion because of Sr's larger atomic radius compared to that of Ca, which introduces additional strain into the lattice [25], [26]. Increased Sr concentrations cause greater lattice distortion due to the differences in ionic radii between Ca and Sr, affecting the local environment and radiative processes.

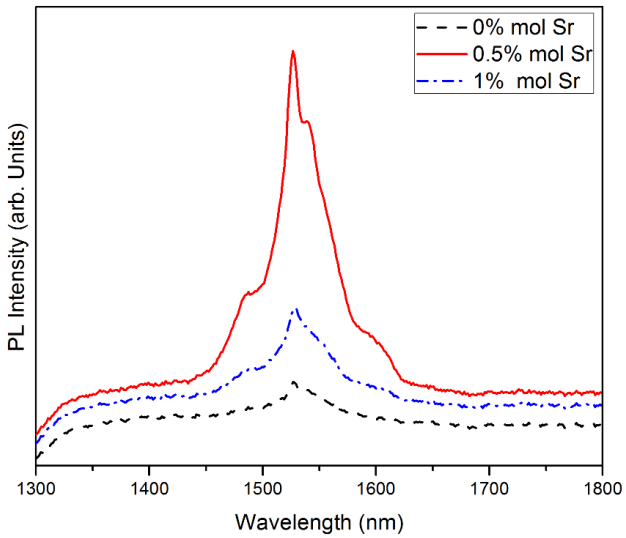

Figure 3. *Photoluminescence spectra of Er-doped Sr-HA/TCP as a function of Sr concentrations annealed at 800 ^oC*

3.4. Effect of annealing temperature and holding time

Photoluminescence (PL) measurements were adopted throughout this study to optically characterize Er-doped Sr-HA. Figure 4 displays the typical PL spectra of Er-doped Sr-HA/TCP. All samples exhibited strong near-infrared emission peaks around 1540 nm, attributed to the transition from the first excited level $^4I_{13/2}$ to the ground state $^4I_{15/2}$ within the 4f electronic configuration. It is important to note that the PL intensity of Er-doped Sr-HA/TCP increased significantly with higher annealing temperatures, peaking at 800°C before decreasing with further increases in temperature. This behavior is attributed to thermal annealing, which promotes the migration of Er ions and removes hydroxyl groups and water molecules from the host material [27], [28]. At 600°C, Er ions are randomly distributed in the host lattice with residual hydroxyl groups, leading to reduced PL intensity. As the annealing temperature rises to 800°C, the PL intensity increases due to the shortened distances between ions and the complete removal of hydroxyl groups and water molecules, facilitating the formation of ion pairs. However, at 900°C, the PL intensity weakens due to Er-Er ion interactions causing quenching. Additionally, the PL characteristics of Er-doped Sr-HA/TCP annealed at 800°C with varying holding times are further illustrated in Figure 5. The emission intensity increased significantly with longer

holding times. From 5 to 30 minutes, the Er ions are typically dispersed randomly throughout the host lattice, whereas at a holding time of 120 min, some Er^{3+} ions become closer to each other, potentially leading to concentration quenching. At a holding time of 60 minutes, the PL spectra of Er-doped Sr-HA/TCP peaked and then declined with an extended holding time of 120 minutes. However, holding times longer than 120 minutes, the emission intensity significantly drops due to Er-Er interactions.

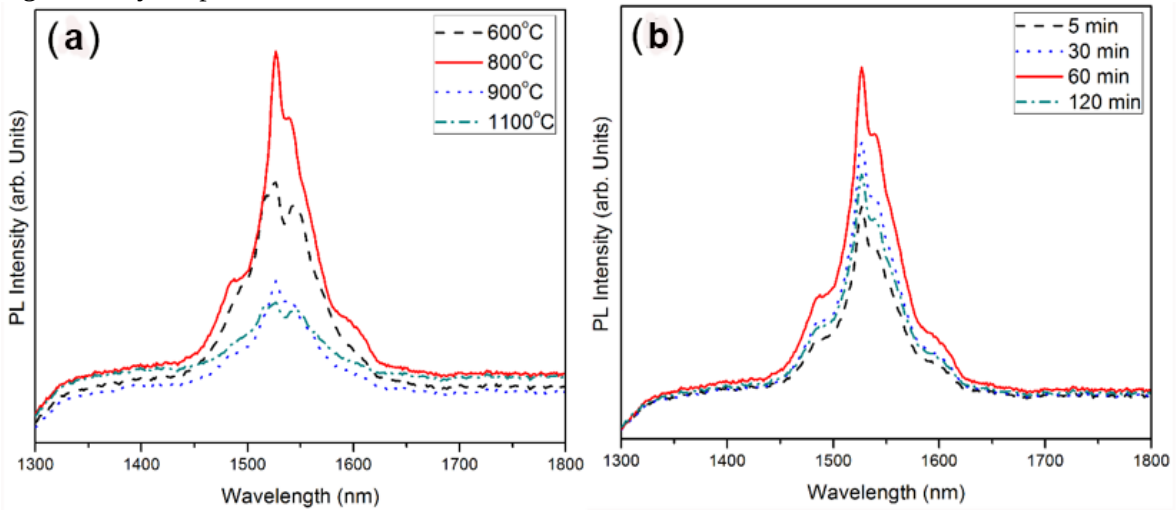

Figure 4. *Photoluminescence spectra of Er-doped Sr-HA/TCP (a) different annealing temperatures, (b) different holding times.*

3.5. Effect of Er concentrations

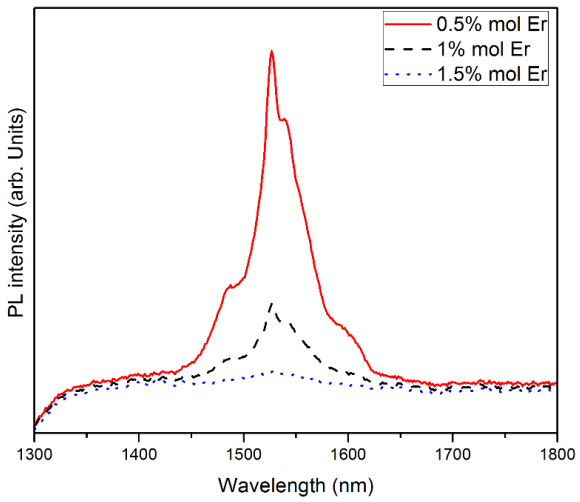

Figure 5. *Photoluminescence spectra of Er doped Sr-HA/TCP as a function of Er concentrations annealed at 800 ^oC*

Figure 5 illustrates the photoluminescence spectra of Er-doped Sr-HA/TCP nanoparticles with varying Er concentrations annealed at 800 ^oC. Notably, the relative PL intensity of the sample changed with varying Er doping concentrations. Figure 5 shows that at 3 doping concentrations of 0.5, 1, and 1.5% mol Er, the PL intensity decreased gradually. Among them, the highest PL intensity was observed at 0.5% mol Er. When Er ions are doped, the Er^{3+} luminescent centers substitute for Ca^{2+} sites, leading to the immediate recombination of many electron-hole pairs and the emission of photons. Consequently, the PL intensity varies depending on the Er concentration.

However, beyond these Er concentrations, the PL intensity decreases due to quenching effects caused by Er^{3+} clustering [29], [30]. In other words, this clearly demonstrates that the dopant concentration strongly influences the luminescence efficiency of Er-doped Sr-HA/TCP.

4. Conclusions

We have shown that the near-infrared light emission of Sr-HA/TCP can be effectively achieved by doping it with rare earth erbium. Specifically, the photoluminescence of Er-doped Sr-HA/TCP exhibits a strong band around 1540nm, which is influenced by various conditions such as the doping concentration ratio of Sr and Er. Additionally, the photoluminescence intensity varies with temperature and sample annealing time. This emission was significantly stronger than that of Er-doped HA/TCP. The improvement in PL is mainly attributed to changes made in the local environment, crystallinity and dopant distribution, indicating potential applications in waveguide telecommunication and biomedicine.

Acknowledgment

This research was funded by the Ministry of Education and Training (MOET) under grant number CT2022.03/CT2022.03.BKA.04

REFERENCES

[1] R. Dahal, C. Ugolini, J. Y. Lin, H. X. Jiang, and J. M. Zavada, "1.54 μm emitters based on erbium doped InGaN p-i-n junctions," *Appl. Phys. Lett*., vol. 97, pp. 141109-141109-3, 2010, doi: 10.1063/1.3499654.

[2] R. Dahal, C. Ugolini, J. Y. Lin, H. X. Jiang, and J. M. Zavada, "Erbium-doped GaN optical amplifiers operating at 1.54 μm," *Appl. Phys. Lett*., vol. 95, pp. 111109-111109-3, 2009, doi: 10.1063/1.3224203.

[3] X. Liu, B. Mei, and G. Tan, "Investigation of the sensitization effect of Yb^{3+} in Yb, Er co-doped $Sr_5(PO_4)_3F$ transparent ceramics: From single-band red up conversion to temperature sensing behavior," *Journal of the European Ceramic Society*, vol. 44, pp. 7855-7866, 2024, doi: 10.1016/j.jeurceramsoc.2024.05.078.

[4] H. Q. Ye, Z. Li, Y. Peng, C. C. Wang, T. Y. Li, Y. X. Zheng, A. Sapelkin, G. Adamopoulos, I. Hernández, P. B. Wyatt, and W. P. Gillin, "Organo-erbium systems for optical amplification at telecommunications wavelengths," *Nature Mater*., vol. 13, pp. 382-386, 2014, doi: 10.1038/nmat3910.

[5] O. Savchyn, R. M. Todi, K. R. Coffey, and P. G. Kik, "High-temperature optical properties of sensitized Er^{3+} in Si-rich SiO_2 – implications for gain performance," *Opt. Mater*., vol. 32, pp. 1274-1278, 2010, doi: 10.1016/j.optmat.2010.04.037.

[6] B. Garrido, C. García, S. Y. Seo, P. Pellegrino, D. Navarro-Urrios, N. Daldosso, L. Pavesi, F. Gourbilleau, and R. Rizk, "Excitable Er fraction and quenching phenomena in Er-doped SiO_2 layers containing Si nanoclusters," *Phys. Rev. B*, vol. 76, pp. 245308-245308-15, 2007, doi: 10.1103/PhysRevB.76.245308.

[7] J. C. G. Bünzli and C. Piguet, "Taking advantage of luminescent lanthanide ions," *Chem. Soc. Rev*., vol. 34, pp. 1048-1077, 2005, doi: 10.1039/B406082M.

[8] Q. Zhong, H. Wang, G. Qian, Z. Wang, J. Zhang, J. Qiu, and M. Wang, "Novel stoichiometrically erbium−ytterbium cocrystalline complex exhibiting enhanced near-infrared luminescenc," *Inorg. Chem*., vol. 45, pp. 4537-4543, 2006, doi: 10.1021/ic051697y.

[9] J. Wu, J. L. Coffer, Y. Wang, and R. Schulze, "Oxidized Germanium as a Broad-Band Sensitizer for Er-Doped SnO_2 Nanofibers," *J. Phys. Chem. C*, vol. 113, pp. 12-16, 2009, doi: 10.1021/jp8080996.

[10] Z. Xia, H. Liu, X. Li, and C. Liu, "Identification of the crystallographic sites of Eu^{2+} in $Ca_9NaMg(PO_4)_7$: structure and luminescence properties study," *Dalton Trans*.. vol. 42, pp. 16588-16595, 2013, doi: 10.1039/C3DT52232F.

[11] J. P. Gittings, C. R. Bowen, A. C. E. Dent, I. G. Turner, F. R. Baxter, and J. B. Chaudhuri, "Electrical characterization of hydroxyapatite-based bioceramics," *Acta Biomaterialia*, vol. 5, pp. 743-754, 2009, doi: 10.1016/j.actbio.2008.08.012.

[12] L. Stipniece, S. Wilson, J. M. Curran, R. Chen, K. S. Ancane, P. K. Sharma, B. J. Meenan, and A. R. Boyd, "Strontium substituted hydroxyapatite promotes direct primary human osteoblast maturation," *Ceramics International*, vol. 47, pp. 3368-3379, 2021, doi: 10.1016/j.ceramint.2020.09.182.

[13] M. S. Collin, A. Sharma, A. Bhattacharya, and S. Sasikumar, "Synthesis of strontium substituted hydroxyapatite by solution combustion route," *Journal of the Indian Chemical Society*, vol. 98, p. 100191, 2021, doi: 10.1016/j.jics.2021.100191.

[14] A. M. Dias, and I. D. N. Canhas, C. G. O. Bruziquesi, M. G. Speziali, R. D. Sinisterra, and M. E. Cortés, "Magnesium (Mg^{2+}), Strontium (Sr^{2+}), and Zinc (Zn^{2+}) Co-substituted Bone Cements Based on Nano-hydroxyapatite/ Monetite for Bone Regeneration," *Biological Trace Element Research*, vol. 201, pp. 2963-2981, 2023, doi: 10.1007/s12011-022-03382-5.

[15]Y. Zhuang, A. Liu, S. Jiang, U. Liaqat, K. Lin, W. Sun, and C. Yuan, "Promoting vascularized bone regeneration via strontium-incorporated hydroxyapatite bioceramic," *Materials & Design*, vol. 234, p. 112313, 2023, doi: 10.1016/j.matdes.2023.112313.

[16] C. Zhang, C. Li, S. Huang, Z. Hou, Z. Cheng, P. Yang, C. Peng, and J. Lin, "Self-activated luminescent and mesoporous strontium hydroxyapatite nanorods for drug delivery," *Biomaterials*, vol. 31, pp. 3374-3383, 2010, doi: 10.1016/j.biomaterials.2010.01.044.

[17] R. E. Ouenzerfi, N. Kbir-Ariguib, M. Trabelsi-Ayedi, and B. Piriou, "Spectroscopic study of Eu^{3+} in strontium hydroxyapatite $Sr_{10}(PO_4)_6(OH)_2$," *J. Lumin*., vol. 85, pp. 71–77, 1999, doi: 10.1016/S0022-2313(99)00149-0.

[18] V. H. Pham, H. N. Van, P. D. Tam, and H. N. T. Ha, "A novel 1540 nm light emission from erbium doped hydroxyapatite/β-tricalcium phosphate through co-precipitation method," *Mater. Lett.*, vol. 167, pp. 145-147, 2016, doi: 10.1. 016/j.matlet.2016.01.002.

[19] B. O. Fowler, E. C. Moreno, and W. E. Brown, "Infra-red spectra of hydroxyapatite, octacalcium phosphate and pyrolysed octacalcium phosphate," *Arch. Oral Bid*., vol. 11, pp. 477-492, 1966, doi: 10.1016/0003-9969(66)90154-3.

[20] F. H. Lin, C. J. Liao, K. S. Chen, and J. S. Sun, "Preparation of high-temperature stabilized β-tricalcium phosphate by heating deficient hydroxyapatite with $Na_4P_2O_7{\cdot}10H_2O$ addition," *Biomaterials*, vol. 19, pp. 1101-1107, 1998, doi: 10.1016/S0142-9612(98)00040-4.

[21] H. Monma, S. Ueno, and T. Kanazawa, "Properties of hydroxyapatite prepared by the hydrolysis of tricalcium phosphate," *J. Chem. Tech. Biotechnol*., vol. 31, pp. 15–24. 1981, doi: 10.1002/jctb.503310105.

[22] A. Mortier, J. Lemaitre, and P. G. Rouxhet, "Temperature-programmed characterization of synthetic calcium-deficient phosphate apatites," *Thermachimia Acta*, vol. 143, pp. 265-282, 1989, doi: 10.1016/0040-6031(89)85065-8.

[23] F. R.O. Silva, N. B. Lima, S. N. Guilhen, L. C. Courrol, and A. H. A. Bressiani, "Evaluation of europium-doped HA/β-TCP ratio fluorescence in biphasic calcium phosphate nanocomposites controlled by the pH value during the synthesis," *J. Lumin*., vol. 180, pp. 177-182, 2016, doi: 10.1016/j.jlumin.2016.08.030.

[24] C. Rosticher, B. Viana, T. Maldiney, C. Richard, and C. Chanéac, "Persistent luminescence of Eu, Mn, Dy doped calcium phosphates for in-vivo optical imaging," *J. Lumin*., vol. 170, pp. 460-466, 2016, doi: 10.1016/j.jlumin.2015.07.024.

[25] S. Ogo, A. Onda, Y. Iwasa, K. Hara, A. Fukuoka, and K. Yanagisawa, "1-Butanol synthesis from ethanol over strontium phosphate hydroxyapatite catalysts with various Sr/P ratios," *J. Catalysis*, vol. 296, pp. 24-30, 2012, doi: 10.1016/j.jcat.2012.08.019.

[26] J. Wu and J. L. Coffer, "Emissive erbium-doped silicon and germanium oxide nanofibers derived from an electrospinning process," *Chem. Mater*., vol. 19, pp. 6266-6276, 2007, doi: 10.1021/cm702226x.

[27] H. Hayash, N. Sugimoto, S. Tanabe, and S. Ohara, "Effect of hydroxyl groups on erbium-doped bismuth-oxide-based glasses for fiber amplifiers," *J. Appl. Phys*., vol. 99, pp. 093105-093105-8, 2006, doi: 10.1063/1.2192267.

[28] X. Feng, S. Tanabe, and T. Hanada, "Hydroxyl groups in erbium-doped germanotellurite glasses," *J. Non–Cryst. Solids*, vol. 281, pp. 48-54, 2001, doi: 10.1016/S0022-3093(00)00429-4.

[29] P. K. Sekhar, A. R. Wilkinson, R. G. Elliman, T.H. Kim, and S. Bhansali, "Erbium emission from nanoengineered silicon surface," *J. Phys. Chem. C*, vol. 112, pp. 20110-20113, 2008, doi: 10.1021/jp808462j

[30] Y. C. Yan, A. J. Faber, H. de Waal, P. G. Kik, and A. Polman, "Erbium-doped phosphate glass waveguide on silicon with 4.1 dB/cm gain at 1.535 μm," *Appl. Phys. Lett*., vol. 71, pp. 2922-2924, 1997, doi: 10.1063/1.120216.